A CONSISTENT KINETICS POROSITY (CKP) MODEL

R.M. Brannon

Sandia National Laboratories, Computational Physics and Mechanics MS 0820, Albuquerque, NM 87185-0820

Abstract. A theory is presented for the mechanical response of porous media to high-strain-rate deformations. The model is "consistent" because each feature is incorporated in a manner that is mathematically compatible with all the other features. Unlike simple p-α models, the onset of pore collapse depends (via a user-adjustable yield function) on the amount of shear present. The elastic part of the strain rate is linearly related to the stress rate, except for nonlinear contributions due to the change in the elastic moduli upon pore collapse. The inelastic part of the strain rate includes parts from plastic deformation of the matrix material, pore nucleation, and phase transformations in the matrix material. The plastic strain rate is taken normal to the yield surface. Consequently, if phase transformation and/or nucleation are simultaneously occurring, the inelastic strain rate will be non-normal to the yield surface. The matrix yield stress is permitted to harden linearly. Plastic volume changes of the matrix material are assumed negligible in comparison to macroscopic volume changes associated with pore collapse. Rate dependence is allowed via an overstress model. The theory has been exercised under a rigorous array of canonical loading paths with special care to ensure sensible response upon unloading and reloading. Results show good progress toward modeling a particular 10% porous ferroelectric ceramic.

INTRODUCTION

The development of deformation-induced porosity or the presence of artificially-induced porosity can significantly affect the mechanical performance of a material. The theory outlined below combines numerous disjoint porosity model features from the literature into a single consistent framework that is designed to be flexible enough to apply to a wide array of porous materials.

THEORY

Rather than quantifying porosity by the pore volume fraction f, we instead use the ratio of pore volume to matrix volume, $\psi \equiv f/(1-f)$. Some other pore models use a distention density ratio defined $\alpha = \rho/\rho_m$, where ρ is density and the subscript "m" denotes the matrix material. Our pore ratio ψ is related to α by $\psi=\alpha-1$. The pore ratio ψ in our equations is at the *unstressed* reference state. It changes only via plastic deformations. The actual loaded porosity *can* change during elastic deformations, but ψ would remain constant.

The bulk and shear moduli, K and G, vary exponentially with the unstressed pore ratio ψ by

$$K = K_m e^{-\kappa_m \psi} \quad \text{where} \quad \kappa_m = \frac{4G_m + 3K_m}{4G_m} \tag{1}$$

$$G = G_m e^{-\gamma_m \psi} \quad \text{where} \quad \gamma_m = \frac{5(4G_m + 3K_m)}{8G_m + 9K_m} \tag{2}$$

We derived the above expressions for γ_m and κ_m by generalizing published low-porosity analytical results[1] to reflect exponential trends in data for ceramics[2]. In our implementation, the user gives the macroscopic bulk and shear moduli, K and G, and the above equations are numerically inverted to infer the matrix moduli K_m and G_m.

The present model is isotropic, and yield is presumed expressible via a user-supplied yield function F that depends on four variables: an equivalent shear stress τ, the pressure p, the pore ratio ψ, and internal state variable(s) ς. A stress state is below yield if

$$F(\tau, p, \psi, \varsigma) < 0 \tag{3}$$

The "strain rate" tensor $\underset{\sim}{\dot{\varepsilon}}$ is decomposed as

$$\dot{\underset{\sim}{\varepsilon}} = \dot{\underset{\sim}{\varepsilon}}_e + \dot{\underset{\sim}{\varepsilon}}_p^G + \dot{\underset{\sim}{\varepsilon}}_p^N + \dot{\underset{\sim}{\varepsilon}}_p^T \tag{4}$$

where $\dot{\underset{\sim}{\varepsilon}}_e$ is the elastic part, while $\dot{\underset{\sim}{\varepsilon}}_p^G$, $\dot{\underset{\sim}{\varepsilon}}_p^N$, and $\dot{\underset{\sim}{\varepsilon}}_p^T$ are the plastic parts due to void growth, nucleation, and phase transformation, respectively.

Stress is linearly related to elastic strain, but the stress *rate* contains terms for the change in moduli as the porosity changes. For example, $p = -K\varepsilon_v^e$, where ε_v^e is the elastic logarithmic volume strain, defined so that $\dot{\varepsilon}_v^e = \text{trace}(\dot{\underset{\sim}{\varepsilon}}_e)$. Applying (1),

$$\dot{p} = -K\,\text{trace}(\dot{\underset{\sim}{\varepsilon}}_e) - \kappa_m p\dot{\psi} \tag{5}$$

Similarly, the stress deviator $\underset{\sim}{\tau}$ is related to the elastic strain deviator, $\underset{\sim}{\varepsilon}'_e$, by $\underset{\sim}{\tau} = 2G\underset{\sim}{\varepsilon}'_e$, so that

$$\dot{\underset{\sim}{\tau}} = 2G\dot{\underset{\sim}{\varepsilon}}'_e - \gamma_m \underset{\sim}{\tau}\dot{\psi} \tag{6}$$

The growth part of the plastic strain rate is taken to be directed normal to the yield surface:

$$\dot{\underset{\sim}{\varepsilon}}_p^G = \dot{\lambda}\,\partial F/\partial \underset{\sim}{\sigma} \tag{7}$$

The proportionality variable $\dot{\lambda}$ is called the plastic segment. It is zero during any interval of elastic loading, and it must be positive during plastic deformation. The numerical implementation of this model constantly monitors to check that $\dot{\lambda} > 0$. Negative values of $\dot{\lambda}$ are permitted only during iterations to put the stress state on the yield surface (the final value of $d\lambda$ must still be positive).

The rates of the internal state variables (if any) are presumed proportional to the plastic segment:

$$\dot{\varsigma} = h\xi\dot{\lambda}, \qquad \text{where } \xi \equiv \left\| \partial F/\partial \underset{\sim}{\sigma} \right\| \tag{8}$$

For linear hardening, h is a user-supplied constant. Our implementation treats the yield stress of the matrix material as an internal state variable.

During an interval of continued plastic deformation, not only must the stress state be on the yield surface, it must also *remain* on the yield surface. Thus, $F=0$ and $\dot{F}=0$, giving

$$\frac{\partial F}{\partial \tau}\dot{\tau} + \frac{\partial F}{\partial p}\dot{p} + \frac{\partial F}{\partial \psi}\dot{\psi} + \frac{\partial F}{\partial \varsigma}\dot{\varsigma} = 0 \tag{9}$$

In the absence of phase transformation, permanent volume changes of the matrix material are neglected in comparison to volume changes that result from pore growth/collapse within the composite. This approximation gives an elegant relationship between the unstressed reference porosity and the total plastic strain rate[3,4]:

$$\dot{\psi} = (1+\psi)\,\text{trace}(\dot{\underset{\sim}{\varepsilon}}_p^G + \dot{\underset{\sim}{\varepsilon}}_p^N), \tag{10}$$

For the present model, we rewrite this as

$$\dot{\psi} = (1+\psi)\,\text{trace}(\dot{\underset{\sim}{\varepsilon}}_p^G) + \dot{\psi}^N \tag{11}$$

where the pore nucleation rate $\dot{\psi}^N$ is proportional to the amount by which an *ad hoc* estimated local stress in the matrix material exceeds a critical value. (Future versions of this model will include fracture damage that will activate well before nucleation.)

The transformation strain is taken proportional to the extent of transformation η so that $\underset{\sim}{\varepsilon}_p^T = \eta\underset{\sim}{\varepsilon}^*$, where $\underset{\sim}{\varepsilon}^*$ is the final strain of transformation (uniaxial in the local domain dipole direction for our ferroelectric ceramic of interest). Nonlinear phase transformation is accomplished by allowing the transformation stress to be a function of the extent of transformation. For our material of interest, data show an increase in the bulk modulus following transformation. Lacking sufficient micromechanical data to the contrary, we have presumed that the macroscopic stiffening is caused by a stiffening of the matrix material, not by a change in the porosity.

The above governing equations can be solved[5] to determine all of the rate quantities, which are then numerically integrated to update the material state.

The above theory is rate independent and has been carefully constructed to ensure consistent kinetics (*e.g.*, the stress remains on/in the yield surface). This consistent kinetics porosity (CKP) theory governs the "equilibrated" state. For high strain rates, we allow the instantaneous stress to differ from the equilibrated stress $\underset{\sim}{\sigma}^{eq}$ by an overstress $\underset{\sim}{\sigma}^{over}$, as illustrated in Fig. 1. The instantaneous stress rate is taken to equal the elastic trial stress rate minus a restoring stress rate that brings the stress back towards the equilibrated stress. The restoring stress rate is proportional to the magnitude of the overstress. Figure 2 shows the shear response to

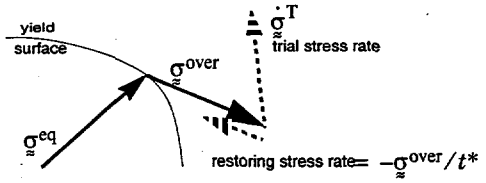

FIGURE 1. Overstress model. The stress is the vector sum of the solid arrows. The stress *rate* is the sum of the dashed vectors.

identical strains applied at *different* rates (see inset). For higher strain rates, the characteristic relaxation time t^* increases the *apparent* yield stress.

Recall that the yield function of Eq. (3) is ideally supplied by the user. Our model has been implemented with a "dearth of data" (DOD) yield function that may be used as a flexible default when measurements of the yield function are unavailable. For our DOD yield function, the yield stress $\bar{\tau}$ of the matrix material is a user input. The macroscopic yield in shear taken to be $\bar{\tau}$ times the solid volume fraction (thus initial yield is less than $\bar{\tau}$ in Fig. 2).

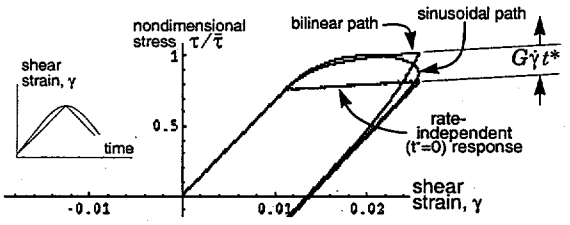

FIGURE 2. Shear response with hardening and rate effects.

The default DOD yield point for pure isotropic volumetric straining is given by the Gurson-Rice[6] implied p-α curve (dashed line in Fig. 3). The solid line in Fig. 3 shows a computed prediction of the CKP model, demonstrating consistency because the pressure always remains on or within this p-α yield curve. The associated pressure vs. volumetric strain shows considerable initial pore collapse. When the pressure is further increased, the slope approaches the bulk modulus of the matrix material.

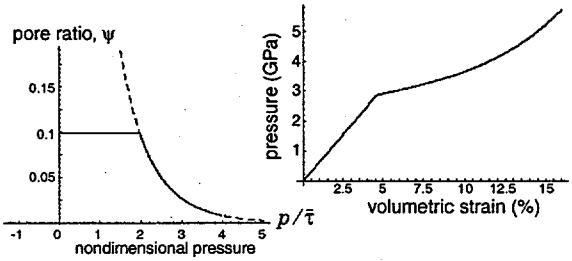

FIGURE 3. CKP model under hydrostatic loading.

For loading that includes both shear and volume change, we allow the shape of the DOD yield surface in τ vs. p space to be interpolated between an ellipse and a circumscribed rectangle (like conventional p-α theory). The major axes of the ellipse or rectangle correspond to the pure shear and volumetric loadings described above. To allow for different yield in tension and compression, the ellipse/rectangle may be shifted along the pressure axis. To allow shear-enhanced compaction (or to compensate for a yield shift), the slope at the midpoint may be altered.

RESULTS AND DISCUSSION

To ensure robustness, a stand-alone test code was developed to exercise the model under strain-controlled paths that were more severe than normally encountered in physical applications. Correct installation of the model into the Sandia wave propagation code ALEGRA[7] was verified by duplicating these single-cell results using ALEGRA's prescribed boundary velocity capability. Comparisons with shock impact experiments are now being conducted. Fig. 4 shows the improved agreement of the CKP model (using a Gurson yield function) with measurements of shock-induced particle velocity for a PZT ferroelectric ceramic. Optimal parameters, alternative yield functions, and mechanical anisotropy (induced by ferroelectric poling) are now being implemented, so the agreement is expected to further improve.

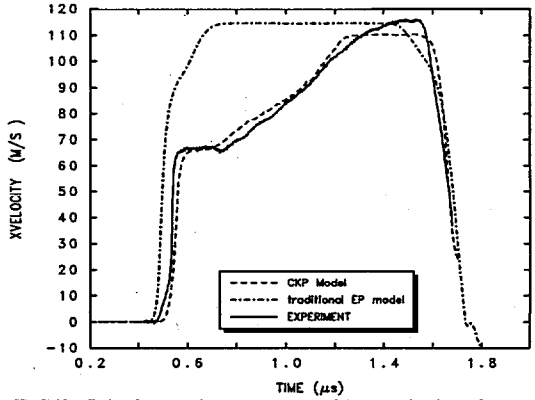

FIGURE 4. Comparison (to date) with velocity interferometer measurements for a conventional elastic-plastic model and for the new CKP pore model (using Gurson's yield function).

For the same ferroelectric ceramic, the parameters that control the phase transformation have been fit to the experimental data[8] shown in Fig. 5. Note that the present model does not include reverse transformation. Fig. 5 also depicts the qualitatively different response of the same material under uniaxial strain ($H \equiv K + \frac{4}{3}G$ is the constrained modulus, σ_A is the axial stress, and σ_L is the lateral stress, which becomes tensile because the lateral strain constraint prevents transformation

contraction). The transformation pressure for this material is well below the yield point, so all of the nonlinearity is due to phase change, not plasticity.

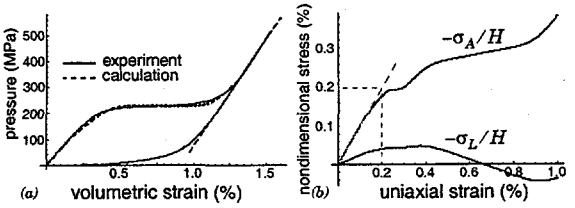

FIGURE 5. Phase transformation for (a) unpoled isotropic strain compression and (b) poled uniaxial strain compression.

Figure 6 shows a verification test of the CKP model under severe uniaxial strain compression followed by extension. The initial slope matches the porous constrained modulus. Yield and pore collapse commences gradually **(B)** and continues until pores have all compressed out **(C)**, beyond which the slope equals the matrix bulk modulus. Release **(D)** is elastic until yield resumes **(E)**. Eventually enough tension builds to nucleate pores **(F)**, which grow **(G)** and cause a stress drop. At recompression **(H)** the elastic slope is shallower due to increased porosity.

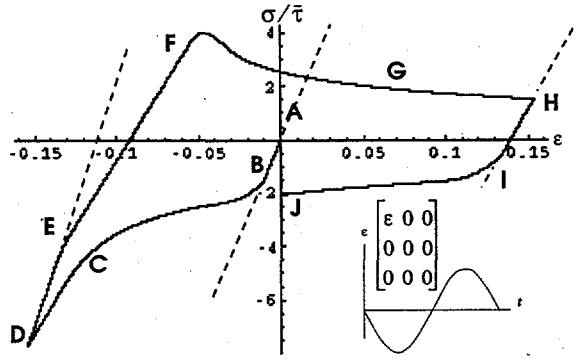

FIGURE 6. CKP prediction of uniaxial strain response. The inset shows the strain vs. time. Elastic slopes are shown dashed.

The DOD yield surface is methodically explored in Fig. 7 under uniaxial strain. *All of the test parameter sets in that figure would predict identical response in hydrostatic compression.* The presence of shear and the shape of the yield surface account for the illustrated differences in uniaxial strain. Specific changes in the stress-strain curve can be realized by more than one possible change in the physical model parameters. Hence, a systematic study of *numerous* measured strain paths is essential to reveal a truly appropriate family of parameters.

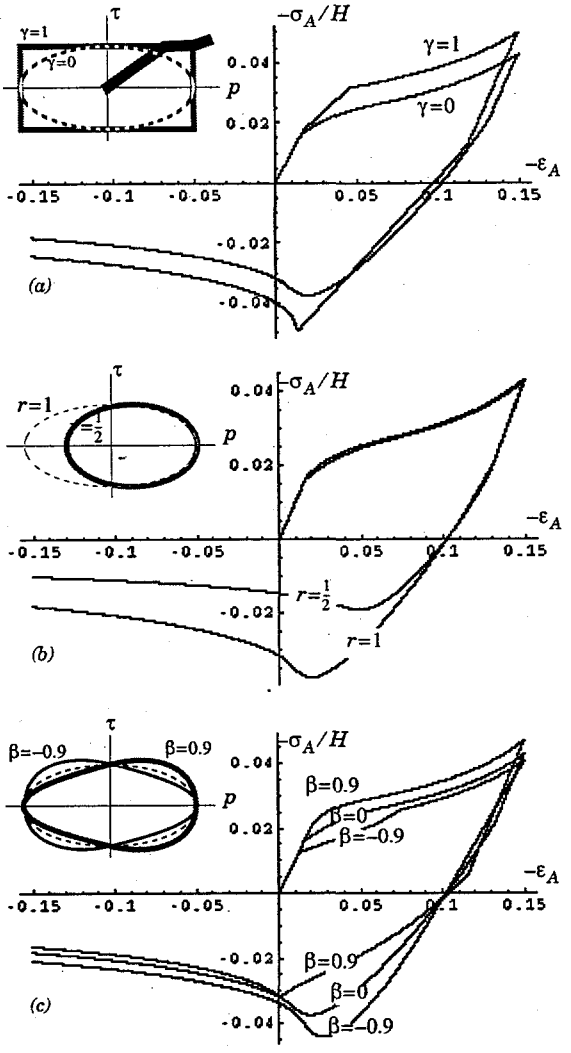

FIGURE 7. DOD yield parameter study for uniaxial strain

ACKNOWLEDGMENTS

Sandia is a multiprogram laboratory operated by Sandia Corporation, a Lockheed Martin Company, for the United States Department of Energy under Contract DE-AC04-94AL85000.

REFERENCES

1. Zhao, Z.Q., Tandon, G.P., and Weng, G.J., *Acta Mech* **76**, p 105 (1989).
2. Rice. R. W., *Porosity of Ceramics*, Marcel Dekker, Inc. (1998).
3. Needleman, A., and Rice, J.R., In *Mechanics of Sheet Metal Forming* (edited by D.P. Koistinen and N.-M. Wang) p237 (1978).
4. Brannon, R.M. and Drugan, W.J., *J. Mech. Phys. Solids* **41**(2), p 297 (1993).
5. Brannon, R.M., Sandia National Laboratories Technical Report in preparation (1999).
6. Gurson, A.L., *J. Engng Mater. Technol.* **99**, 2 (1977).
7. Summers, R.M., Peery, J.S., Wong, M.K., Hertel, E.S., Trucano, T.G., and Chhabildas, L.C., International Journal of Impact Engineering, pp. 779-788 (1997).
8. Zeuch, D.H., Montgomery, S.T., Carlson, L.W., and Grazier, J.M. Sandia National Laboratories report SAND99-0635 (1999).

DISCLAIMER

DISCLAIMER

Portions of this document may be illegible in electronic image products. Images are produced from the best available original document.